

Magnet Design Report

Quadrupole magnet Q8

Author	Checked by – date	Approved by – date
Davide Castronovo		

Table of Contents

1	INTRODUCTION.....	3
1.1	ACRONYMS AND ABBREVIATIONS.....	3
2	REQUIREMENTS AND DESIGN GUIDELINES.....	3
3	MAGNETS DESIGN.....	4
3.1	INTRODUCTION	4
3.2	POWER CONVERTER MAXIMUM CURRENT	4
3.3	MAGNET PARAMETERS.....	6
3.4	MAGNET YOKE LAYOUTS.....	6
3.5	COIL DESIGN.....	7
4	MAGNETIC FIELD CALCULATION	8
4.1	POLE TIP DESIGN.....	8
4.2	2D5 SIMULATIONS.....	10
4.3	HARMONIC OPTIMIZATION.....	11
4.4	2D5 HARMONIC OPTIMIZATION	11
4.5	3D SIMULATIONS.....	13
4.6	3D HARMONIC OPTIMIZATION	14
5	Q8 SUMMARY	16
5.1	CONCEPTUAL 3D MODEL.....	16
5.2	Q5 MAGNETIC PERFORMANCES.....	17
6	ANNEX.....	18
6.1	MATERIAL USED FOR MAGNETIC SIMULATIONS	18
6.2	QUADRUPOLE MODEL.....	18
6.3	REFERENCES	18

1 INTRODUCTION

The last part of the Accelerator-to-Target (A2T) section of the ESS accelerator contains six high-strength quadrupole magnets for beam focusing and transport to the target in a straight section. These quadrupoles are normal-conducting and operate in DC mode. This document describes the conceptual design of these quadrupoles, which are referred to as type Q8.

1.1 ACRONYMS AND ABBREVIATIONS

Acronym	Explanation
DC	Direct Current
PC	Power Converter
GFR	Good Field Region
FFT	Fast Fourier Transform
GUI	Graphical User Interface
CAD	Computer Aided Design
ABS	Absolute Value
Pw	Power

2 REQUIREMENTS AND DESIGN GUIDELINES

Since these magnets have a large vacuum chamber, i.e. the aperture diameter is large, special attention has been paid to the ampere-turns calculations. Another attention has been paid to limit, in a reasonable way, the overall dimensions of the yoke.

In order to make feasible also the realization of the coils cooled by water, the maximum current value has been set both to reduce the number of turns as well as to minimize the coil overall dimensions.

More in detail, to minimize as much as possible the power consumptions, Q8 must adopt conductors that have a cross section area such as to keep the maximum current density lower than 4.5 A/mm^2 . At the same time, the conductors must have a cooling channel with a diameter sufficiently large in order to reduce the required liquid velocity and thus limiting the pressure drop in the cooling circuit.

To obtain the required total pressure drop ($< 5 \text{ Bar}$), the number of branches have been set and the liquid inlet and outlet interfaces must be defined.

To minimize the eddy current in the iron during the magnet cycling reset or the setting of the current value, the yoke will be made of laminated steel sheets with a thickness of 1.0 mm.

Table 1 reports the requirements for Q8 as reported in DOORS.

Table 1: **Q8** DOORS requirements

<i>ID</i>	<i>Parameter</i>		<i>value</i>	<i>unit</i>
4647	Overall length	\leq	1000	mm
4659	Bore diameter	\geq	126	mm
4649	Nominal magnetic length	\geq	800	mm
4650	Nominal integrated field gradient	$=$	7.8	T
4651	Operation range	$=$	$0.5 \div 7.8$	T
4652	Maximum integrated gradient	\geq	8.2	T
4653	Good field region radius	\geq	45	mm
4656	Multiple content B_n / B_2 ($n = 3 \div 10$)	$<$	± 0.1	%

3 MAGNETS DESIGN

3.1 INTRODUCTION

The magnetic designs started with a pre-design where all the parameters were calculated by theoretical formulas and excel work-sheets. In order to estimate further real 3D parameters such as magnetic length, yoke saturation and magnet inductance, 3D electromagnetic simulations had been run.

After the pre-design, the final magnetic design optimized the multipole components and the field distribution in order to reach all the specifications within the required ranges.

For the electromagnetic simulations and optimizations the software packages VF Opera Tosca, ESTECO modeFRONTIER and Mathworks Matlab have been used.

3.2 POWER CONVERTER MAXIMUM CURRENT

During the Q8 pre-design, several ampere-turns ratios have been evaluated in order to estimate the yoke overall dimension and the cooling circuit feasibility.

Using for Q8 the same maximum current of Q5, Q6 and Q7 (200 Ampere), the calculated ampere-turns value require at least 88 turns. Unfortunately, with the use of this number of turns, for each coil, the resulting total length of the conductor (about 170 m) leads an excessive pressure drop in the cooling circuit.

In order to make feasible the use of a cooling circuit with no more than 4 branches (only one for each coil), all these pre-designs have used a square conductor section (Cond.WH) with a sufficiently big cooling channel diameter (Cond. \emptyset).

Figure 1 shows and compares different quadrupole pre-designs based on different maximum current values.

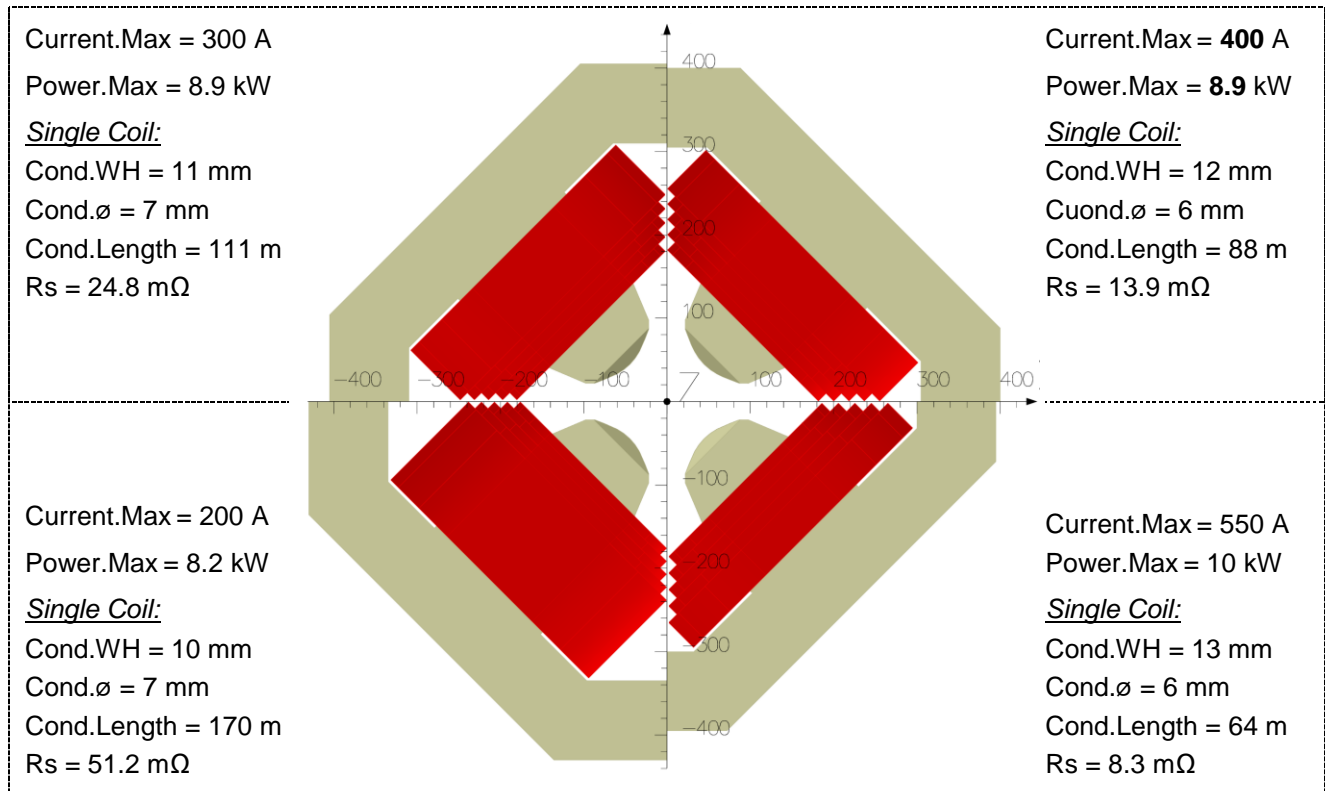


Figure 1: Q8 pre-designs comparison

As is possible to see, with the same ampere-turns excitation, the different maximum current values do not comport very different quadrupoles in terms of overall dimensions and power consumptions.

However, by comparing the most interesting cases of 200 A and 400 A, it can be concluded that the 400 A one is preferable since the coils have half the windings (less cost and greater reliability), the conductor section has a wider minimum thickness (stronger structure and conductor terminations) and the yoke is smaller (the total weight is considerably lower).

Since the Q5, Q6 and Q7, have the maximum excitation current of 200 A, the choice of 400 A (instead of 300 A or higher) for Q8 could make it possible to use, for the network connections between the PCs and the Quads, the same cable cross-section (120 mm²) with two of them in parallel per polarity.

3.3 MAGNET PARAMETERS

Table 2 lists magnet parameters and performances calculated by VF Opera 3D.

Table 2: Magnet parameters and performances

Parameters			unit
Aperture radius	=	126	mm
Yoke overall width and height	=	800	mm
Good field region radius r_0	=	45	mm
Yoke length	=	755	mm
Coils overall length	\leq	940	mm
Magnetic length L_{eff} at nominal I_c	\geq	807	mm
Maximum integrated gradient	=	8.79	T (Tm)
Content B_n / B_2 (with $n = 6, 12$ and 18) at r_0	$<$	0.005	%
Inductance	=	83.6	mH

3.4 MAGNET YOKE LAYOUTS

Table 3 lists all yoke parameters. Note that the yoke weight was calculated by the typically value of the packing factor, which is 0.98.

Table 3: Yoke parameters

Parameters		unit
Type	Four quadrants	
Yoke	Laminated	
Simulated material	VF Opera - tenten	
Simulated packing factor	97	%
Yoke overall width or height	800	mm
Yoke length	755	mm
Yoke volume	244	dm ³
Yoke mass (calculated by $0.98 \cdot \rho_{Fe}$)	1850	kg

In order to reduce the eddy current effect (during the possible startup, the reset cycling or the setting of the current value) it's preferable that the yokes are made of laminated steel sheets of 1.0 mm thickness that are glued together. The recommended steel type will be cold-rolled, final annealed, no grain-oriented electrical steel. The $B(H)$ curve of such a material shall be better or equal to the $B(H)$ curve used for the magnetic field calculations (VF Opera "tenten", see Table 8). The steel strips are pre-coated on both sides with a thin

layer (5 to 8 μm) of epoxy resin. This layer provides the required surface insulation between the laminations and serves at the same time as a bonding agent between them. After stacking and curing, the packing factor¹ of each quadrant shall be greater than or equal to 97 % (low margin respect the typically value of 98%).

3.5 COIL DESIGN

The coils conductor shall be made of high conductivity (OFHC-type) copper. The wire shall be wrapped by two consecutive layers of insulating tapes; the first one of Kapton® polyamide, and the second one of fiberglass, for a total insulation thickness of about 0.5 mm. The coils shall be vacuum-impregnated using a radiation-resistant thermosetting epoxy resin. The final insulation must be able to withstand a suitable test voltage.

The coils will be made of a copper conductor with a cross section of 12 x 12 mm and with a cooling channel diameter of 6 mm; the resulting conducting area is of $\sim 115 \text{ mm}^2$.

The proposed coils geometry is simpler race track type with a total of 44 turns arranged on 6 turns on width.

Figure 2 shows the proposed coil winding and the coil model defined in VF Opera.

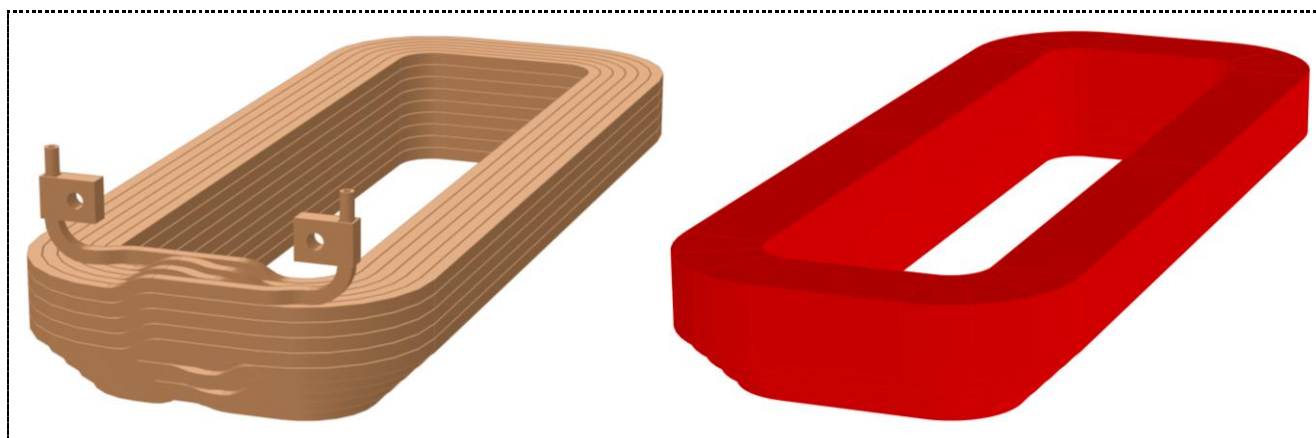


Figure 2: Q8 coil winding and Opera model.

This geometry is well defined by the standard conductor models and for this reasons the real harmonic contributions, due to the coils, will be very similar to the calculated ones.

It should be noted that, due to the required conductor cross section, the pole width inside the coil, that has been optimize in terms of yoke saturation, is little more than necessary to allow transitions on one transversal side.

¹ The packing factor is defined as the ratio of the mass of the steel of the laminated yoke quadrant and the mass of a solid yoke quadrant of the same volume and of the same material density.

Table 4 lists all coil parameters and provides an overview of all relevant power converter and cooling system parameters. Note that the minimum required coolant flow is calculated at the maximum required current I_{RMax} so that a temperature rise of 25°C is obtained.

Table 4: Coil parameters, on parenthesis the values at the minimum required coolant flow

Parameters		unit
Type	Racetrack	
Cooling	demineralized water	
Conductor cross section	12 x 12 mm - hole Ø 6 mm = 115	mm ²
Number of turns for one coil	44	#
Space between coil and yoke	12	mm
Maximum current density j	3.48	A/mm ²
Conductor length for one coil	88.1	m
Resistance for one coil at 22°C	13.3	mΩ
Coil overall length	940	mm
Mass for one coil	~ 95	Kg
PC maximum required current I_{RMax}	371	A
Coolant total flow (<i>minimum required</i>)	8.7 (4.6)	l/min
Cooling power dissipation at I_{RMax}	7.6 (7.9)	kW
Cooling branches number	4	#
Coolant temperature rise at I_{RMax}	12.7 (25.0)	°C
Coolant velocity on each coil	1.3 (0.7)	m/s
Coolant pressure drop	3.8 (1.2)	bar

The coil parameter calculations assumed a resistivity of $1.72 \times 10^{-8} \Omega m$ at 20°C. Due to the relatively high current density, the coils have to be water-cooled. Each coil shall be equipped with two thermal switches for protection against overheating. The thermal switches must be positioned on the outlet connection of each coil. In order to reduce the total pressure drop (< 5 bar), the cooling circuit will have four branches, one for each coil.

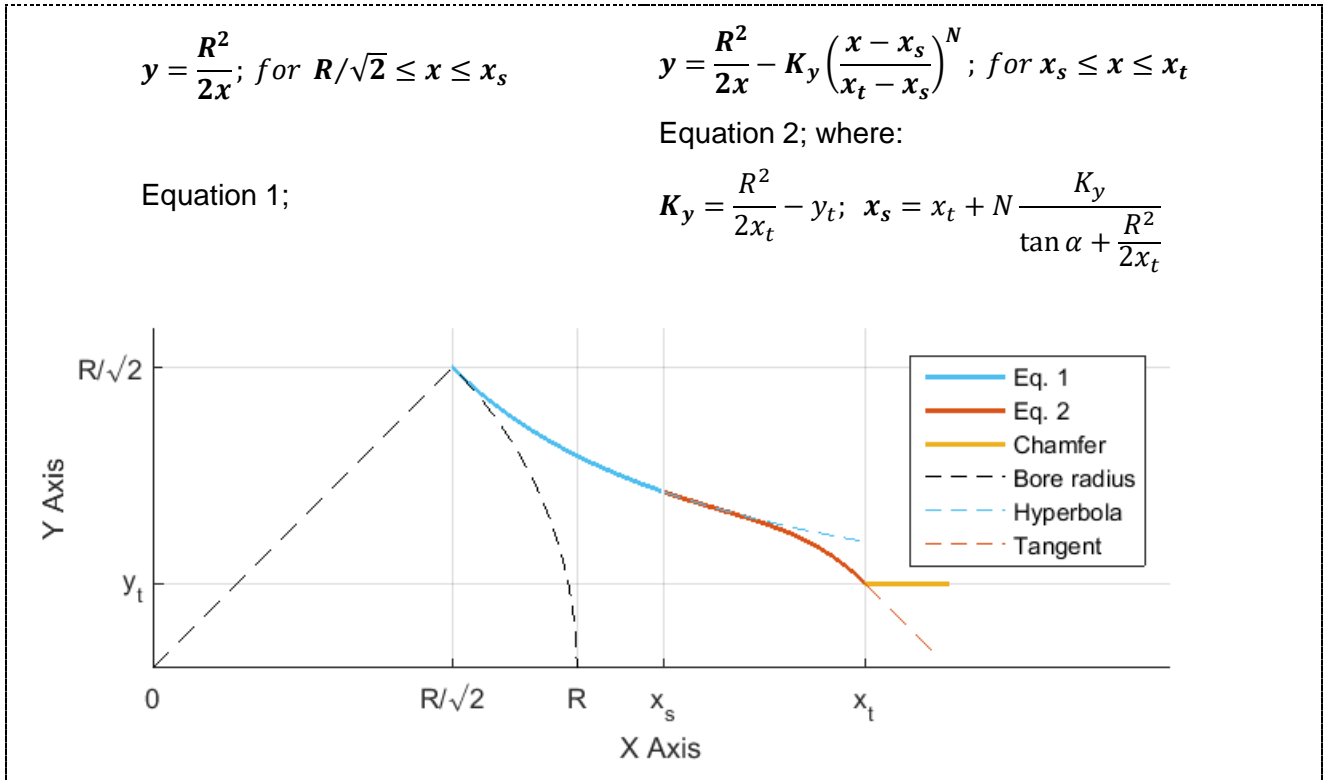
4 MAGNETIC FIELD CALCULATION

4.1 POLE TIP DESIGN

The Q8 pole profile has been defined by the same equation set (with the same type of parameters) used for Q5, Q6 and Q7. The possible Q8 pole profile has been defined

adjusting in a suitable way the available parameters. Table 5 lists the equations and shows a nominal plotting.

Table 5: Pole profile equations and plot



It should be noted that the pole tip profile is divided in two parts defined by two equations: the first one is simply a hyperbola; the second one is the sum of a hyperbola and an exponential. This type of equation has the advantage of being able to define very different curves with the lowest number of parameters. Only three parameters are needed in this particular design: the side point $p_t(x_t, y_t)$, the angle α of the tangent at p_t and the order of the exponential N . These three parameters define also the coordinates of x_s which is the limit between the ranges of the two equations in the x domain.

Since the quadrupole pole profile is made not only by the pole tip but also by the transition between the tip and the sides into the coil, three other parameters are used to define this part: the length of the chamfer ΔX_{ch} , the angle β of the transition and the pole width W_{pole} inside the coil.

One of the purposes of this parametrization was to allow the optimization of the pole profile without any impact on the final yoke dimensions. In fact, the setting of the listed parameters will change only the geometry of the pole termination whether the yoke frame is mastered only by the coil geometry and dimensions.

The goal was to decrease, as much as possible, the transversal dimension, and consequently the quantity of iron. For what concern the gaps between the poles shimming, past experience in quadrupole designs [1] have shown that parallel chamfers between the poles locally decreases the iron saturation and increases the field quality in the required excitation ranges. Furthermore, well-defined gaps obtained in this way are very advantageous when assembling and testing the four quadrant yoke parts.

4.2 2D5 SIMULATIONS

In order to run the optimization of the parameters with faster simulations, Opera 3D has been employed in a pseudo bi-dimensional way, a kind of 2.5D, that we have named 2D5. Since the quadrupoles are symmetric with respect to the xy-plane and the line $y = x$, the 2D5 simulation consists in a 3D simulation of only one eighth of a central slice of the yoke 1 mm thick (a single lamination sheet). In this way the 2D5 and 3D simulations are performed with the same finite elements algorithms and can be defined by the same list of commands (the Opera *.comi) for a better correspondence between the 2D5 and the 3D meshing and final results. The imposed boundary condition of the magnetic flux lines are perpendicular to the x-axis, tangential to the line $y = x$ and tangential to both the lamination sheet surfaces. The yoke material is defined with the BH curve mentioned in section 3.4 without packing factor.

Figure 3 shows the 2D5 simulation models defined in Opera 3D.

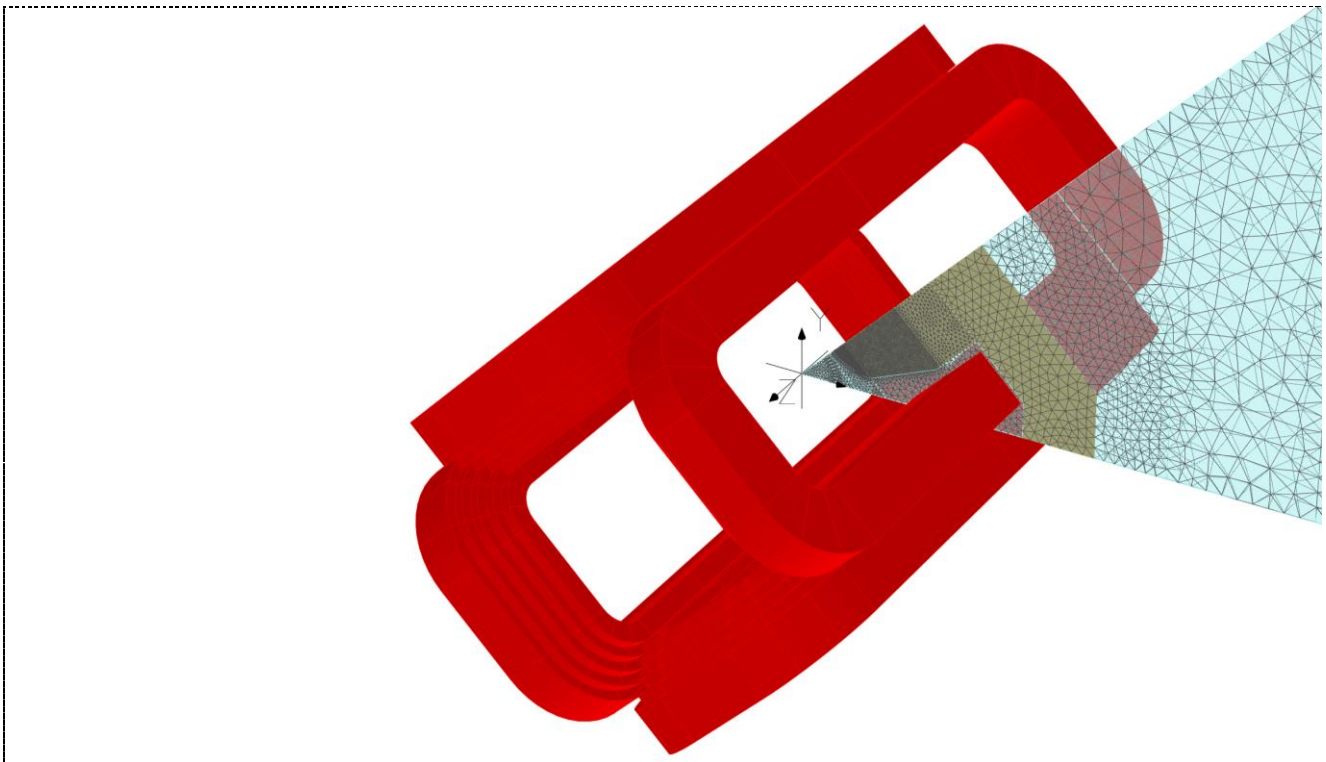


Figure 3: Q8 2D5 model defined in Opera 3D

4.3 HARMONIC OPTIMIZATION

In the 2D5 and 3D simulations, the harmonic content of the magnetic flux density is evaluated calculating the FFT components of the values/integrals of the field around a circle/cylinder defined by the GFR radius.

In order to reduce as much as possible the numeric error, all the simulation models include a GFR cylinder of air. In this way, the points needed for the harmonic calculation are defined by the mesh itself. This method increases the final accuracy since the required field values are included in the finite element calculation and are not affected by a post geometrical interpolation. More precisely, the GFR cylinder is an n-sided prism with a defined angular step. The fields calculated on its edges are mathematically post processed in a range of 2^n to delete the FFT noise.

The goal of the harmonic optimization was to minimize the B_6 and B_{10} components. Given that the simulated models are radially one eighth (a cylinder from 0° to 45°), all the other components (except of course for B_2 , and in particular for B_4 and B_8) can give an estimation of the numeric error. The 2D5 optimizations were assumed completed when B_6 and B_{10} were comparable or lower than the other relative and not possible multipoles (B_4 and B_8).

4.4 2D5 HARMONIC OPTIMIZATION

The pole profile parameters were optimized via 2D5 simulations.

Thanks to the fact that these models are very fast (about 2 minutes for each one), the optimizations have been obtained running Opera under the Esteco modeFRONTIER workflow runner. Figure 4 shows the modeFRONTIER workflow page.

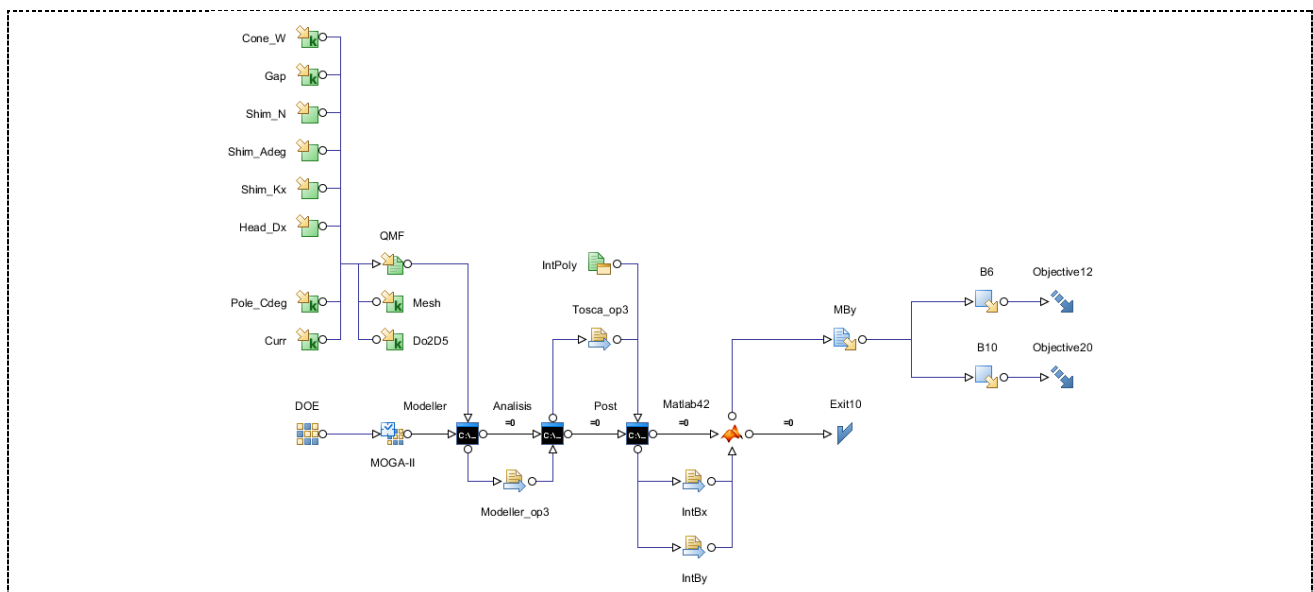


Figure 4: ESTECO modeFRONTIER workflow page

All the parameter ranges have been discretized with steps not smaller than 50 μm for the lengths and 1° for the angles. The main optimization has been done with an equivalent excitation of 375 A.

Figure 5 and Figure 6 show, respectively, the B_6 and B_{10} 2D5 optimization results and the final Q8 pole profile, while Table 6 lists the relative parameter values.

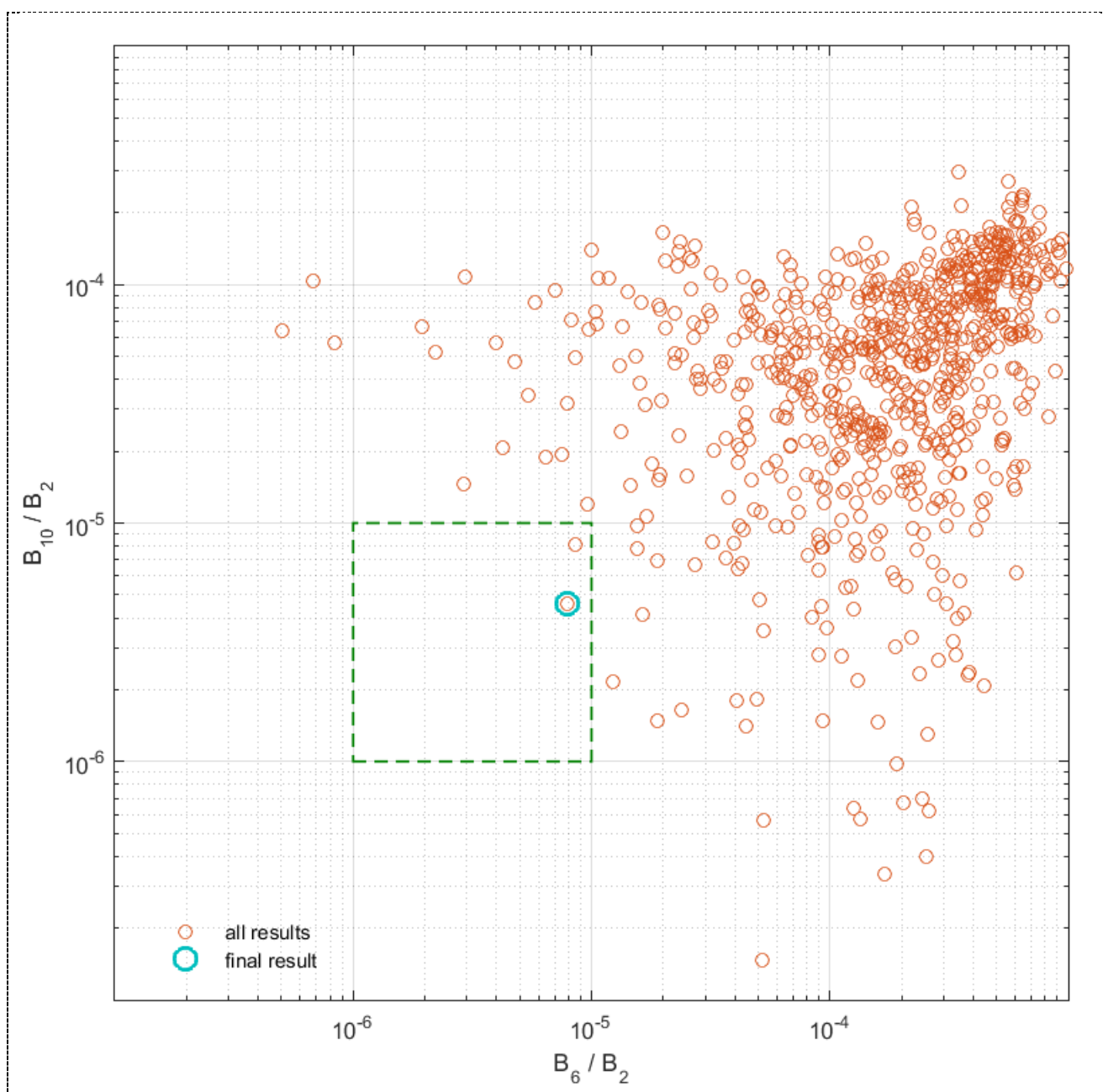


Figure 5: Q8 2D5 harmonic optimization results

Table 6: Q8 final pole profile parameters

Parameter unit	R mm	x_t mm	y_t mm	α deg	N #	ΔX_{Ch} mm	β deg	W_{pole} mm
Q8	63.0	86.6	22	-23	2	11.1	23	180

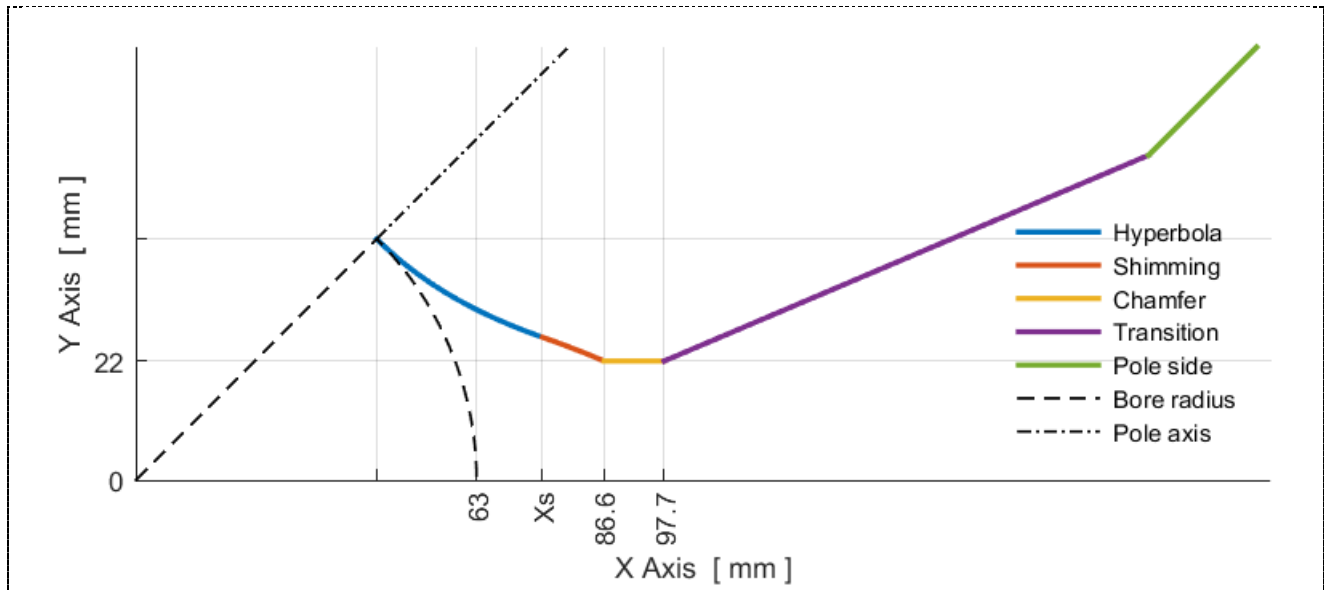


Figure 6: Q8 final pole profile geometry

4.5 3D SIMULATIONS

The 3D simulations have been used for pre-design and 3D harmonic optimization.

In the pre-design, the tridimensional calculations help the evaluation of the magnetic length, the ampere-turns performances and magnet inductance.

Since the quadrupoles have a big aperture, the harmonic effect of the fringe field is not negligible and the final magnetic models need a 3D harmonic optimization.

The Opera 3D models use the same symmetry adopted in the 2D5 simulations (the XY plane and the line $y = x$), plus the longitudinal symmetry on the plane YZ. In this way the simulated model is one-sixteenth ($1/16^{th}$) of the whole quadrupole. The yoke material is defined via the BH curve mentioned in section 3.4 with a packing factor of 97%. As mentioned in section 3.5, the 3D coil models reproduce exactly the real winding of the conductor. The current density is defined including the intra-coils insulation thickness.

Figure 7 shows the Opera 3D models of Q8 yoke, coils and GFR air cylinder. The other air regions are hidden.

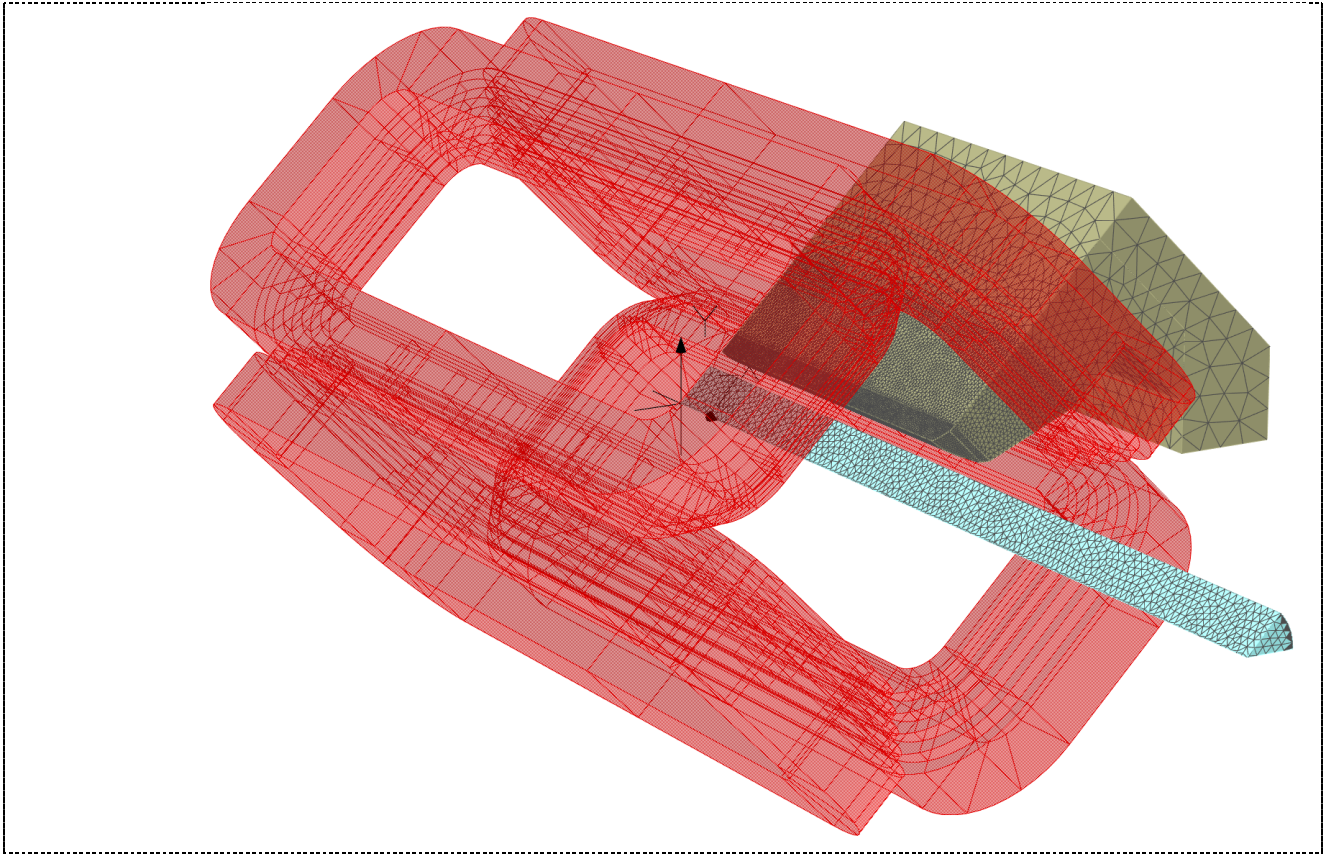


Figure 7: Q8 3D model (1/16th) defined in Opera 3D; yoke, coils and GFR air cylinder.

4.6 3D HARMONIC OPTIMIZATION

Having optimized the pole profiles with the 2D5 method, the 3D stage of the design process will adjust one further parameter, namely the angle of the vertical chamfer of the pole **Ch_θ** . The height of the vertical chamfer **Ch_Δ** is fixed and equal to the height of the hyperbola when the pole profile has no shimming. Since the 3D models need heavier calculations than the 2D5 models, different meshing sizes are evaluated in order to study more thoroughly the final angle of the vertical chamfer.

Figure 8 shows the B_6 and B_{10} Opera 3D simulation results.

For the final 3D model, the vertical chamfer has been set with an angle **Ch_θ** of 40 deg. The height of the vertical chamfer **Ch_Δ** is 14.8 mm.

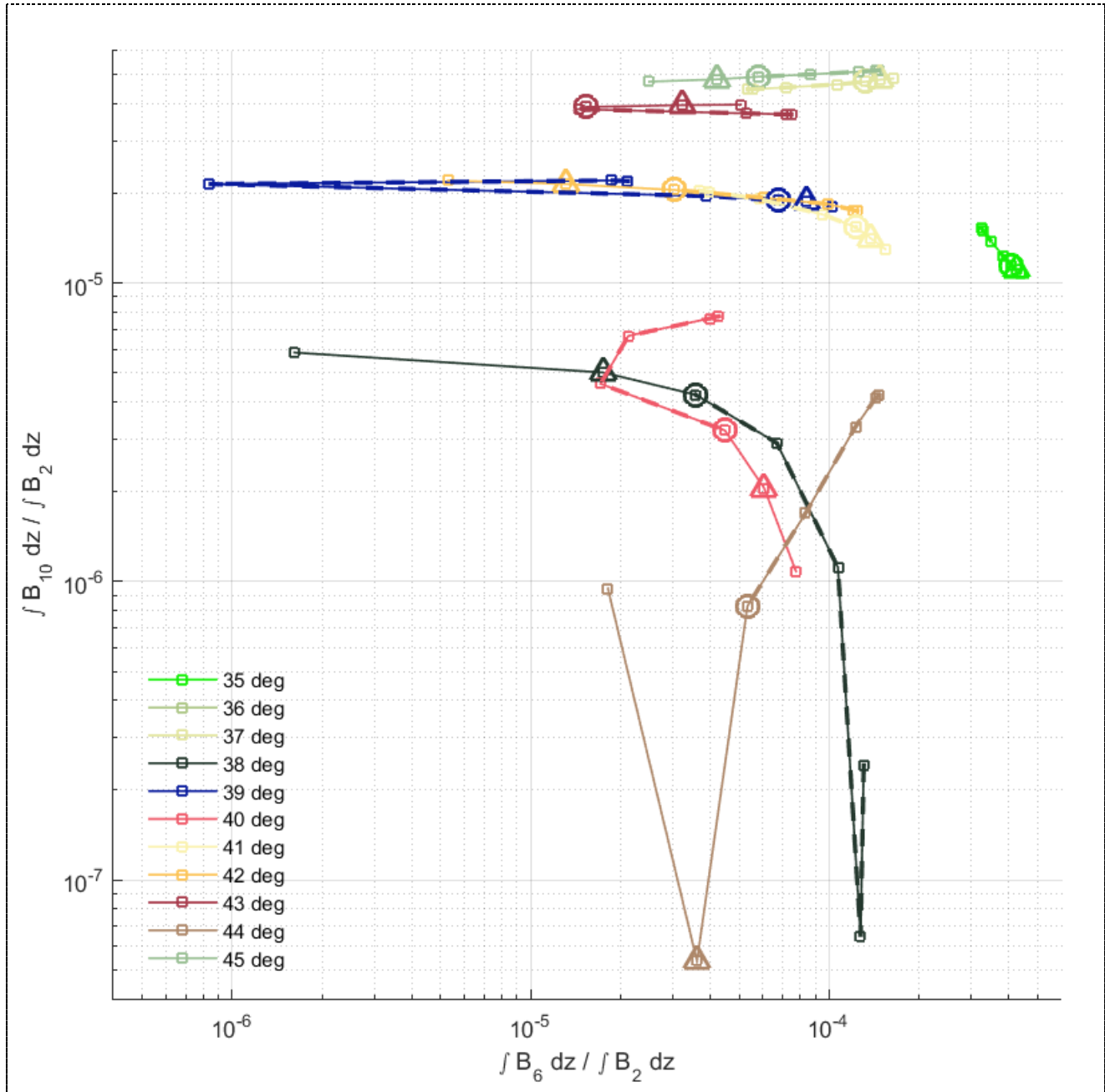


Figure 8: $\int B_6 dz$ and $\int B_{10} dz$ 3D simulation results, from 20 to 400 A (Markers at $\int B_2 dz$ nominal max & max request: ≈ 350 A & ≈ 375 A)

5 Q8 SUMMARY

5.1 CONCEPTUAL 3D MODEL

The Q8 conceptual model include the base yoke quadrants, the coils overall shape and the proposed coil conductor windings.

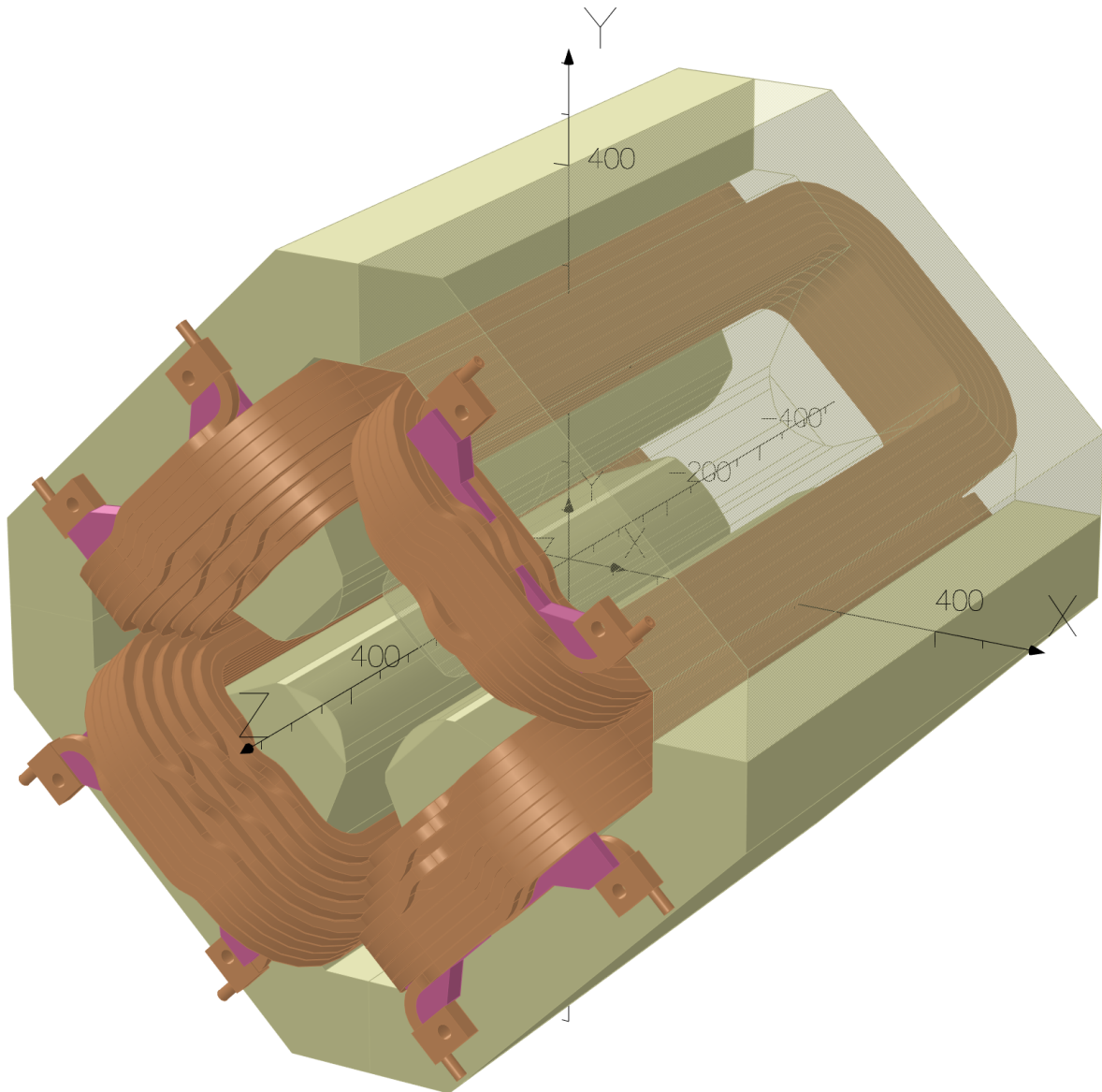


Figure 9: Q8 conceptual model

The yoke frame could be modified in order to increase the supporting surface and defined the closing system. Since the yoke has a sufficient length, the electrical connection box and the cooling circuit manifolds (inlet and outlet) could be positioned on the same side.

5.2 Q5 MAGNETIC PERFORMANCES

In order to obtain consistent results, the Q8 magnetic performances are calculated by Opera 3D for several excitation current values on the same model and exactly the same post processing. The meshing used for this simulation series is higher than the one used for the vertical chamfer optimization and the relative harmonic results are accordingly slightly different. Table 7 lists the Q8 magnetic performances.

Table 7: Q8 magnetic performances; Gradient \mathbf{G} at $r_0 = 45$ mm

	$\mathbf{Curr} [A]$	$\int \mathbf{G} [T]$	$L_{eff} [mm]$	$\mathbf{sat} [\%]$	$\int \mathbf{G}_2 [T]$	$\int \mathbf{G}_6 / \int \mathbf{G}_2$	$\int \mathbf{G}_{10} / \int \mathbf{G}_2$
	400	8.79	803	0.86	8.7944	7.801e-5	1.137e-5
	375	8.29	805	0.60	8.2928	6.713e-5	1.134e-5
	350	7.77	807	0.42	7.7721	5.725e-5	1.131e-5
	300	6.70	810	0.21	6.6978	4.060e-5	1.123e-5
	200	4.48	812	0.05	4.4848	1.871e-5	1.104e-5
	100	2.25	813	0.01	2.2450	8.515e-6	1.085e-5
	50	1.12	813	0.00	1.1226	7.151e-6	1.081e-5
	20	0.45	813	0.02	0.4490	7.152e-6	1.088e-5

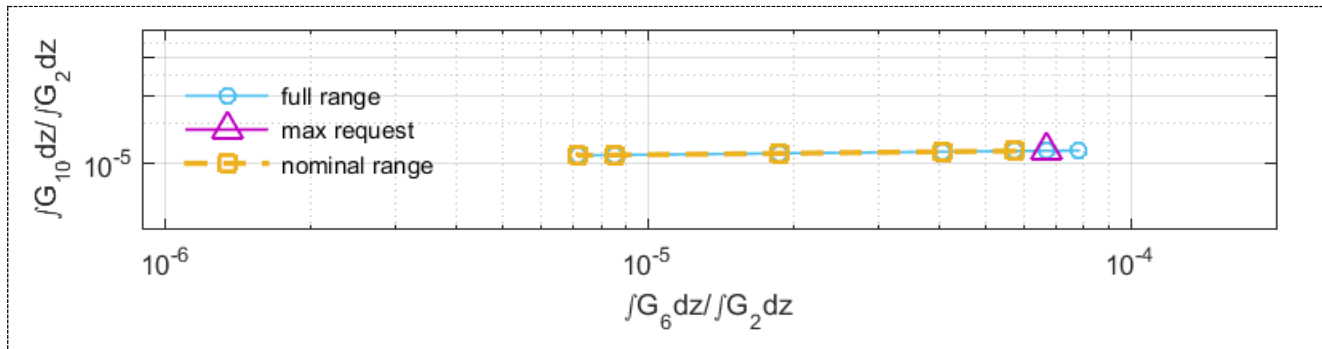


Figure 10: Q8 final model; B_6 and B_{10} multipoles simulation results (higher meshing)

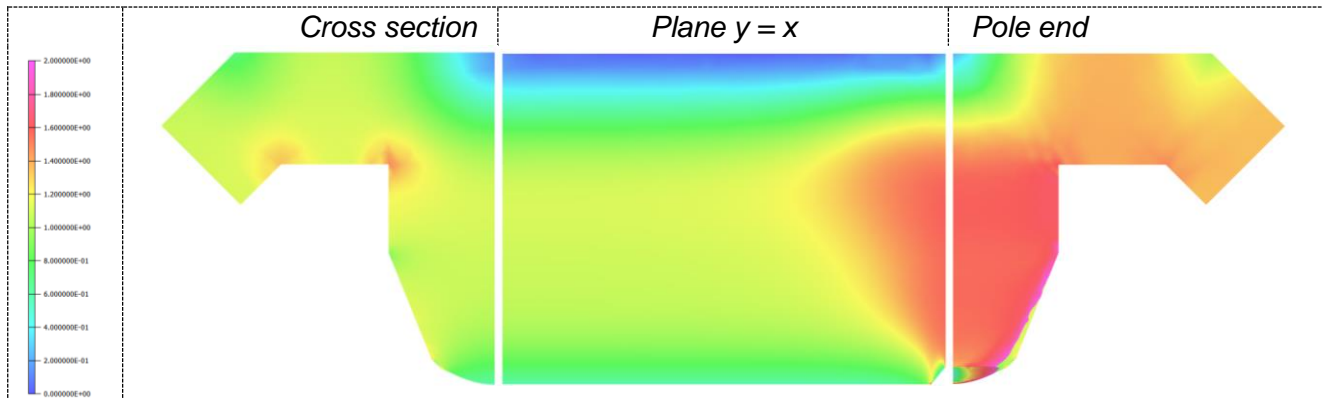


Figure 11: B_{mod} yoke ($1/16^{th}$) distribution at 350 A (nominal maximum), colored bar from 0 to 2 Tesla

6 ANNEX

6.1 MATERIAL USED FOR MAGNETIC SIMULATIONS

The material used for the magnetic simulation is based on the Opera “tenten” data.

Table 8 lists the relative $B(H)$ data.

Table 8: $B(H)$ data of the steel type used for magnetic field simulation

B [Gauss]	H [Oersted]
0	0
5757	2.09
6800	2.5
7918	3.02
8949	3.63
9921	4.365
10821	5.248
11640	6.31
12373	7.586
13021	9.12
13586	10.96
14074	13.18
14494	15.85
15171	22.91
15451	27.54
15955	39.8
16455	57.54
17019	83.18
17679	120.23
18045	144.5
18432	173.8
18831	208.9
19236	251.2
19636	301.99
20022	363.08
20384	436.5
20713	524.8
21003	630.95
21251	758.7
21461	912
21646	1096.5
21869	1318.3
22137	1584.9
22458	1905

6.2 QUADRUPOLE MODEL

The quadrupole 3D model could be exported in the step file format. The following page reports the base drawing of the model.

6.3 REFERENCES

[1] D. Castronovo et al., “The FERMI@Elettra Magnets”, IPAC 2011, San Sebastian, Spain, WEPO003

